JCI The Journal of Clinical Investigation

Divergent requirement for Gαs and cAMP in the differentiation and inflammatory profile of distinct mouse Th subsets

Xiangli Li, … , Paul A. Insel, Eyal Raz

J Clin Invest. 2012;122(3):963-973. https://doi.org/10.1172/JCI59097.

Research Article **Immunology**

cAMP, the intracellular signaling molecule produced in response to GPCR signaling, has long been recognized as an immunosuppressive agent that inhibits T cell receptor activation and T cell function. However, recent studies show that cAMP also promotes T cell–mediated immunity. Central to cAMP production downstream of GPCR activation is the trimeric G protein Gs. In order to reconcile the reports of divergent effects of cAMP in T cells and to define the direct effect of cAMP in T cells, we engineered mice in which the stimulatory Gα subunit of Gs (Gαs) could be deleted in T cells using CD4-Cre (*Gnas*$^{\Delta CD4}$). *Gnas*$^{\Delta CD4}$ CD4$^+$ T cells had reduced cAMP accumulation and Ca^{2+} influx. In vitro and in vivo, *Gnas*$^{\Delta CD4}$ CD4$^+$ T cells displayed impaired differentiation to specific Th subsets: Th17 and Th1 cells were reduced or absent, but Th2 and regulatory T cells were unaffected. Furthermore, *Gnas*$^{\Delta CD4}$ CD4$^+$ T cells failed to provoke colitis in an adoptive transfer model, indicating reduced inflammatory function. Restoration of cAMP levels rescued the impaired phenotype of *Gnas*$^{\Delta CD4}$ CD4$^+$ T cells, reinstated the PKA-dependent influx of Ca^{2+}, and enhanced the ability of these cells to induce colitis. Our findings thus define an important role for cAMP in the differentiation of Th subsets and their subsequent inflammatory responses, and provide evidence that altering cAMP levels in CD4$^+$ T […]

Find the latest version:

https://jci.me/59097/pdf

Divergent requirement for Gαs and cAMP in the differentiation and inflammatory profile of distinct mouse Th subsets

Xiangli Li,[1] Fiona Murray,[1,2] Naoki Koide,[1] Jonathan Goldstone,[1] Sara M. Dann,[1,3] Jianzhong Chen,[1] Samuel Bertin,[1] Guo Fu,[4] Lee S. Weinstein,[5] Min Chen,[5] Maripat Corr,[1] Lars Eckmann,[1] Paul A. Insel,[1,2] and Eyal Raz[1]

[1]Department of Medicine and [2]Department of Pharmacology, UCSD, La Jolla, California, USA. [3]Department of Internal Medicine, Department of Microbiology, University of Texas Medical Branch, Galveston, Texas, USA. [4]Department of Immunology and Microbial Science, The Scripps Research Institute, La Jolla, California, USA. [5]Metabolic Diseases Branch, National Institute of Diabetes and Digestive and Kidney Diseases, NIH, Bethesda, Maryland, USA.

cAMP, the intracellular signaling molecule produced in response to GPCR signaling, has long been recognized as an immunosuppressive agent that inhibits T cell receptor activation and T cell function. However, recent studies show that cAMP also promotes T cell–mediated immunity. Central to cAMP production downstream of GPCR activation is the trimeric G protein Gs. In order to reconcile the reports of divergent effects of cAMP in T cells and to define the direct effect of cAMP in T cells, we engineered mice in which the stimulatory Gα subunit of Gs (Gαs) could be deleted in T cells using CD4-Cre (*Gnas*$^{\Delta CD4}$). *Gnas*$^{\Delta CD4}$ CD4$^+$ T cells had reduced cAMP accumulation and Ca^{2+} influx. In vitro and in vivo, *Gnas*$^{\Delta CD4}$ CD4$^+$ T cells displayed impaired differentiation to specific Th subsets: Th17 and Th1 cells were reduced or absent, but Th2 and regulatory T cells were unaffected. Furthermore, *Gnas*$^{\Delta CD4}$ CD4$^+$ T cells failed to provoke colitis in an adoptive transfer model, indicating reduced inflammatory function. Restoration of cAMP levels rescued the impaired phenotype of *Gnas*$^{\Delta CD4}$ CD4$^+$ T cells, reinstated the PKA-dependent influx of Ca^{2+}, and enhanced the ability of these cells to induce colitis. Our findings thus define an important role for cAMP in the differentiation of Th subsets and their subsequent inflammatory responses, and provide evidence that altering cAMP levels in CD4$^+$ T cells could provide an immunomodulatory approach targeting specific Th subsets.

Introduction

The stimulatory Gα subunit (Gαs) of the trimeric G protein Gs plays a central role in GPCR-mediated signal transduction by coupling the receptors to the activation of adenylyl cyclase (AC) and increased synthesis of cAMP (1). Increases in cAMP can inhibit T cell function, e.g., blunting CD4$^+$ T cell activation, proliferation, and production of certain cytokines, such as IFN-γ and TNF-α (2, 3). In contrast to these data, cAMP has also been shown to stimulate inflammation by promoting Th17 cell expansion (4–6). For example, the mucosal adjuvant cholera toxin (CT), via a cAMP-dependent mechanism, provokes Th17 immune response at mucosal sites (7).

To help resolve such discrepant findings regarding the role of cAMP in CD4$^+$ Th cell differentiation and function, we generated conditional knockout mice whose CD4$^+$ T cells lack the gene for Gαs (*Gnas*$^{\Delta CD4}$ mice) and thus have decreased production of cAMP. We found that CD4$^+$ T cells isolated from *Gnas*$^{\Delta CD4}$ mice had reduced cAMP levels, decreased Ca^{2+} influx, and weak Th17 and Th1 responses but normal Th2 and Treg responses both in vitro and in vivo. Our data thus suggest that cAMP in CD4$^+$ T cells is proinflammatory by altering the differentiation and activation of Th subsets.

Results

Gnas$^{\Delta CD4}$ *CD4$^+$ T cell mice have reduced IL-17 and IFN-γ production.* GPCR-mediated increase in intracellular cAMP requires the activation of AC by Gαs (3). We used the Cre-loxP system to generate mice with a deletion of *Gnas* (the gene that encodes Gαs) targeted to T cells (8). The targeted genetic deletion of Gαs with CD4-Cre occurs at the CD4$^+$CD8$^+$ stage. Consequently, we found that both peripheral CD4$^+$ and CD8$^+$ T cells from *Gnas*$^{\Delta CD4}$ mice lacked Gαs expression (Figure 1A). *Gnas*$^{\Delta CD4}$ and WT mice had similar numbers of CD4$^+$ and CD8$^+$ T cells and a similar percentage of effector memory (CD44^{hi}CD62L^{lo}) and naive (CD44^{lo}CD62L^{hi}) CD4$^+$ and CD8$^+$ T cells (Supplemental Figure 1, A–E; supplemental material available online with this article; doi:10.1172/JCI59097DS1), indicating that the loss of Gαs did not affect T cell development overall.

Figure 1B shows that compared with WT CD4$^+$ cells, CD4$^+$ T cells from *Gnas*$^{\Delta CD4}$ mice, have blunted cAMP accumulation in response to the AC activator forskolin and the agonists of Gαs-coupled GPCRs PGE_2 and isoproterenol in the presence of the phosphodiesterase 4 (PDE4) inhibitor rolipram. Rolipram was used based on the high expression of PDE4B and the greater ability of PDE4 inhibitors to increase cAMP compared with other family-specific PDE inhibitors in CD4$^+$ T cells (Supplemental Figure 2). Reduced cAMP accumulation in *Gnas*$^{\Delta CD4}$ CD4$^+$ T cells in response to AC activation by forskolin is consistent with the observation that Gαs is necessary for maximal forskolin-stimulated AC activation (9). GPCR-stimulated cAMP levels were similar in CD11c$^+$ bone marrow–derived dendritic cells (BMDCs) from *Gnas*$^{\Delta CD4}$ and WT mice (Figure 1C), consistent with a T cell–specific deletion of Gαs (Figure 1A).

Assessment of the cytokine profile of CD4$^+$ T cells isolated from the *Gnas*$^{\Delta CD4}$ mice revealed lower levels of IL-17A, IL-22, and IFN-γ production upon stimulation with anti-CD3/CD28 Abs compared with the responses of WT CD4$^+$ T cells (Figure 1D). Despite the change in the cytokine profile, we observed no significant differ-

Conflict of interest: The authors have declared that no conflict of interest exists.
Citation for this article: *J Clin Invest.* 2012;122(3):963–973. doi:10.1172/JCI59097.

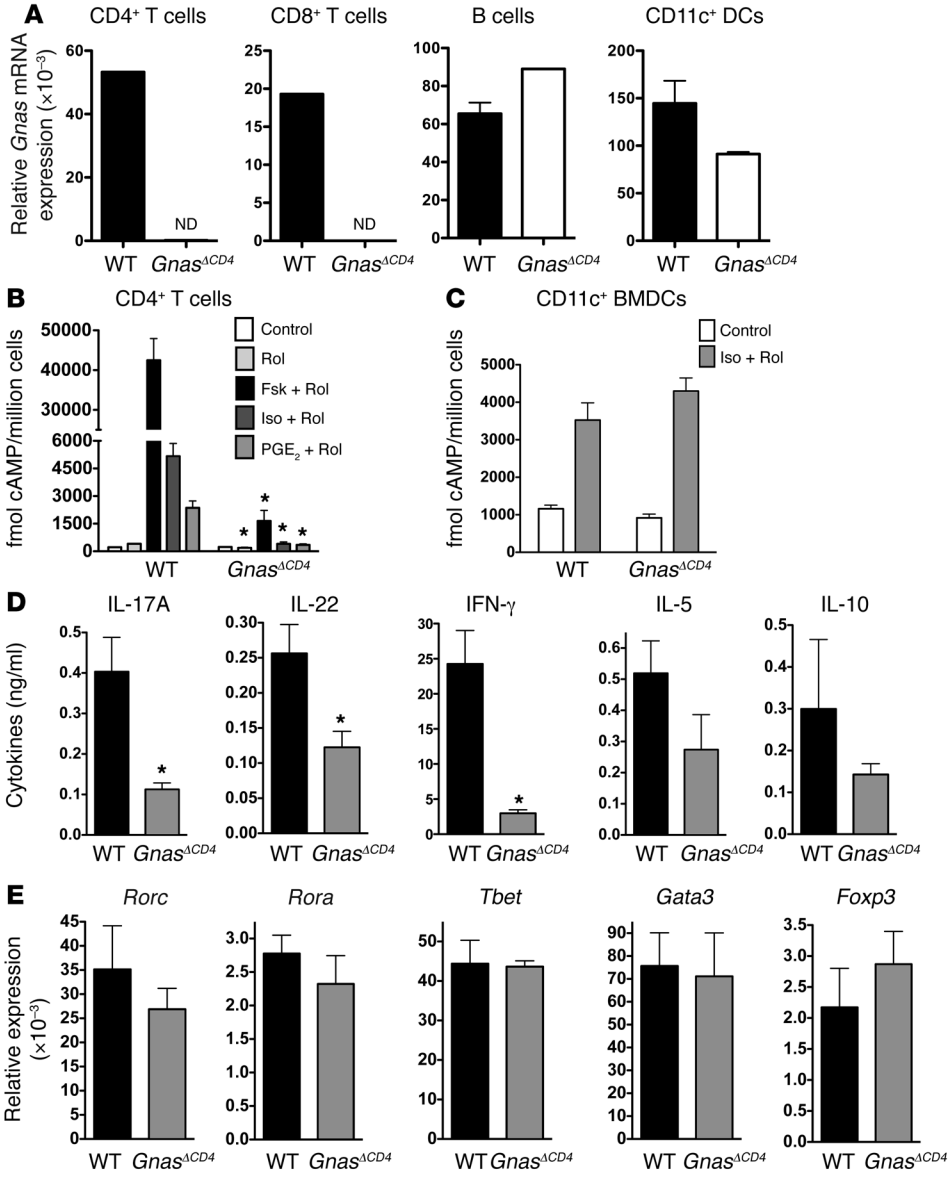

Figure 1
Reduced cAMP, IL-17, and IFN-γ production in $Gnas^{\Delta CD4}$ CD4+ T cells. (**A**) Deficient expression of *Gnas* mRNA in $Gnas^{\Delta CD4}$ CD4+ and CD8+ T cells. Messenger RNA was prepared from sorted splenic CD4 T cells ($TCR\beta^+CD4^+$), CD8+ T cells ($TCR\beta^+CD8^+$), B cells ($TCR\beta^-CD19^+$), and DCs ($CD11c^+TCR\beta^-CD19^-$). ND, not detected. (**B**) Reduced cAMP accumulation in CD4+ T cells of $Gnas^{\Delta CD4}$ mice. cAMP accumulation was assessed in CD4+ T cells from WT and $Gnas^{\Delta CD4}$ mice treated with vehicle, forskolin (Fsk), isoproterenol (Iso), or PGE_2 in the presence of the PDE4 inhibitor rolipram (Rol). Data are mean ± SEM, $n = 3$, from a representative experiment of 3 with similar results; $^*P < 0.05$, $Gnas^{\Delta CD4}$ compared with WT cells under the same conditions. (**C**) cAMP accumulation in $CD11c^+$ BMDCs from WT and $Gnas^{\Delta CD4}$ mice treated with vehicle or isoproterenol in the presence of rolipram. (**D**) Reduced Th17 and Th1 cytokine in $Gnas^{\Delta CD4}$ CD4+ T cells. Splenic CD4+ T cells from WT or $Gnas^{\Delta CD4}$ mice were stimulated by anti-CD3/CD28 Abs for 72 hours, and the levels of cytokines were determined (ELISA). $n = 7$–8 for each group from 2 experiments with similar results; $^*P < 0.05$. (**E**) mRNA levels of transcription factors in $Gnas^{\Delta CD4}$ CD4+ T cells. Messenger RNA was prepared from cells used in **D** to assess transcription factors by quantitative PCR. The expression levels (**A** and **E**) were normalized to the expression of the *Rplp0* housekeeping gene.

ences in the mRNA levels of the Th17- and Th1-lineage commitment transcription factors *Rorc* and *Tbet* (Figure 1E), suggesting that lineage commitment is not altered in $Gnas^{\Delta CD4}$ mice. Functionally $Gnas^{\Delta CD4}$ mice also had reduced ability to clear *Citrobacter rodentium* compared with WT mice despite similar bacterial loads at 1 week after infection (Supplemental Figure 1F). Also, the CD4+ T lymphocytes from the colon lamina propria (LPLs) of $Gnas^{\Delta CD4}$ infected mice had a lower expression of $IL\text{-}17A^+$ cells and $IFN\text{-}\gamma^+$ cells (Supplemental Figure 1G).

We also evaluated the possible contribution of $CD8^+$ T cells and BMDCs from $Gnas^{\Delta CD4}$ mice to CD4+ T cell function. As shown in Supplemental Figure 3, deletion of Gαs in these cells did not affect OVA-specific CD4+ T cells responses.

$Gnas^{\Delta CD4}$ mice do not mount an antigen-specific Th17 response. The data generated with anti-CD3/CD28 Ab stimulation (Figure 1D) suggest a defect in Th17 cytokine production by $Gnas^{\Delta CD4}$ CD4+ T cells. To determine antigen-specific Th17 immune responses in $Gnas^{\Delta CD4}$ CD4+ T cells, we used in vitro and in vivo immunization protocols with OVA and CT (7). Figure 2A shows that compared with control OT-2 cells, OT-2/$Gnas^{\Delta CD4}$ CD4+ T cells differentiated in vitro had reduced production of Th17 cytokines (IL-17A and IL-22). Furthermore, CD4+ T cells isolated from the spleens of in vivo OVA/CT-immunized WT mice, but not $Gnas^{\Delta CD4}$ mice, mounted OVA-specific IL-17A and IL-22 responses (Figure 2B). Consistent with previous data (7), we did not detect OVA-specific IL-17F and IL-21 production in OVA-stimulated CD4+ T cell cultures (Figure 2, A and B). Collectively, the data in Figures 1 and 2 provide evidence that Gαs-mediated signaling in CD4+ T cells is necessary for Th17 response.

$Gnas^{\Delta CD4}$ CD4+ T cells fail to induce colitis. Adoptive transfer of naive WT CD4+ T cells into $Rag1^{-/-}$ recipients provokes colitis, because CD4+ T cells acquire a colitogenic Th1 and/or a Th17 phenotype (10, 11). We investigated whether $Gnas^{\Delta CD4}$ CD4+ T cells develop this colitogenic phenotype in the adoptive transfer model. The transfer of WT CD4+ T cells into $Rag1^{-/-}$ mice produced greater loss in body weight (Figure 3A), higher disease activity index

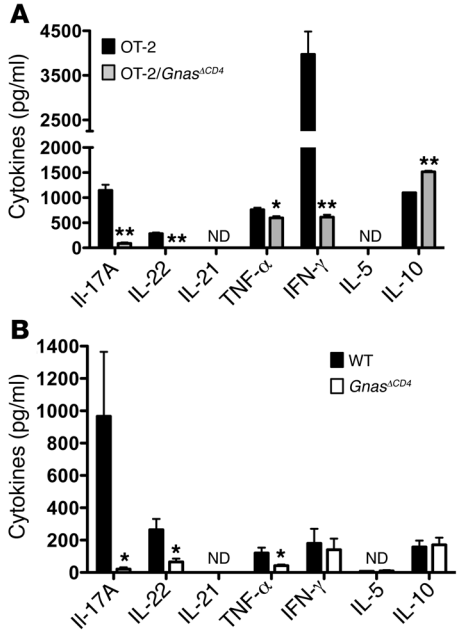

Figure 2

Gαs-mediated signaling in CD4+ T cells promotes antigen-specific Th17 cell response. (**A**) Decreased IL-17A and IL-22 in *Gnas*$^{\Delta CD4}$ CD4+ OT-2 cells. Enriched splenic CD4+ T cells from OT-2 or OT-2/*Gnas*$^{\Delta CD4}$ mice were cocultured with WT CD11c+ splenic DCs at a 2:1 ratio for 5 days in the presence of class II OVA–derived peptide. The OT-2 cells were restimulated by plate-bound anti-CD3/28 Abs for 24 hours, and the cytokine levels were determined (ELISA). Data are mean ± SEM; $n = 3$; $^*P < 0.05$, $^{**}P < 0.01$. (**B**) Gαs-mediated signaling in CD4+ T cells promotes OVA-specific Th17 cell response in vivo. WT or *Gnas*$^{\Delta CD4}$ mice immunized orally with CT and OVA. After 42 days, the splenocytes were collected and restimulated with OVA for 3 days in vitro, and the levels of cytokines were determined in the supernatants (ELISA). Data are mean ± SEM; $n = 6$, from 2 experiments; $^*P < 0.05$ by Mann-Whitney *U* test.

(Figure 3B), and more severe colonic inflammation than the transfer of *Gnas*$^{\Delta CD4}$ CD4+ T cells (Figure 3C). Consistent with these findings, we found lower levels of IL-17A, IL-22, and IFN-γ in the colonic explants of recipients transferred with *Gnas*$^{\Delta CD4}$ CD4+ T cells (Figure 3D). However, we were unable to recover sufficient *Gnas*$^{\Delta CD4}$ CD4+ T cells from LPLs as compared with WT mice for detailed studies. *Gnas*$^{\Delta CD4}$ CD4+ T cells isolated from recipients' spleens 4 weeks after transfer displayed fewer IFN-γ+, IFN-γ+IL-17A+, and TNF-α+ CD4+ T cells than did cells isolated from the spleen of *Rag1*$^{-/-}$ mice that received WT CD4+ T cells (Figure 3E). These results provide further evidence for the contribution of Gαs to Th1 and Th17 differentiation but do not exclude a defect in the cells' ability to migrate to the colon.

Gnas$^{\Delta CD4}$ *CD4+ T cells display reduced Th17 and Th1 cell differentiation in vitro*. Figures 1–3 indicate a role for Gαs in the acquisition of Th17 and Th1 effector functions. To further elucidate the role of Gαs in Th subset differentiation of CD4+ T cells, we used an in vitro differentiation system for each Th subset: after FACS sorting of naive CD4+ T cells from the spleens of WT and *Gnas*$^{\Delta CD4}$ mice, we cultured the cells for 4 days under Th17, Th1, Th2, and Treg polarization conditions; stimulated the cells with PMA/ionomycin; and assessed (by flow cytometry) the intracellular levels of IL-17, IFN-γ, IL-4, and Foxp3 (Figure 4). WT CD4+ T cells had a 2.8-fold greater increase (i.e., 41.6% vs. 14.9%) in IL-17–producing cells (Th17) in response to an IL-6/TGF-β differentiation protocol (12) and a 22-fold increase in IL-17–producing cells (Th17) in response to an IL-6/IL-23/IL-1 differentiation protocol (13) compared with *Gnas*$^{\Delta CD4}$ mice (Figure 4A), thus demonstrating a role for Gαs in Th17 differentiation. Furthermore, WT CD4+ T cells had an 81-fold increase in IFN-γ–producing cells (Th1, Figure 4B) but a similar number of IL-4–producing cells (Th2, Figure 4C) compared with *Gnas*$^{\Delta CD4}$ CD4+ T cells. We also observed no significant differences in Tregs between WT and *Gnas*$^{\Delta CD4}$ mice: Foxp3+ expression (Figure 4D) and stability (Supplement Figure 4A), IL-10 production (Supplemental Figure 4B), and the suppressive effect on WT CD4+ T cell proliferation (Supplemental Figure 4C) were similar in Tregs from WT and *Gnas*$^{\Delta CD4}$ mice. Taken together, these data suggest that Gαs in CD4+ T cells regulates Th17 and Th1, but not Th2 or Treg, cell differentiation.

cAMP restores the ability of Gnas$^{\Delta CD4}$*CD4+ T cells to promote Th17 and Th1 differentiation*. Since *Gnas*$^{\Delta CD4}$ CD4+ T cells have blunted cAMP accumulation, we hypothesized that addition of exogenous cAMP would reverse the effects of the genetic deletion. We thus treated *Gnas*$^{\Delta CD4}$ FACS-sorted naive CD4+ T cells cultured under Th17 and Th1 polarization conditions with 8 bromo-cAMP (8Br-cAMP), a cell-permeable cAMP analog, and found (Figure 5A) a 2.1-fold increase in IL-17+ cells in response to the IL-6/TGF-β differentiation and a 3.3-fold increase in response to the IL-6/IL-23/IL-1β differentiation protocol. The increase in IL-17+ cells by 8Br-cAMP was dose dependent (Supplemental Figure 5A). 8Br-cAMP treatment of WT CD4+ T cells increased Th17 cells by 50% (Figure 5A) under both Th17 polarization conditions and increased IL-17+TNF-α+ cells by 50%–200% in both WT and *Gnas*$^{\Delta CD4}$ CD4+ T cells (Figure 5B). 8Br-cAMP increased *Gnas*$^{\Delta CD4}$ CD4+IFN-γ+ T cells by 5.8-fold (Figure 5C) and of *Gnas*$^{\Delta CD4}$ IFN-γ+TNF-α+ cells by 5.2-fold (Figure 5D) but did not alter either cell population in WT CD4+ T cells. 8Br-cAMP did not increase IL-4+ cells (Th2) or Foxp3+ cells (Tregs) in either WT or *Gnas*$^{\Delta CD4}$ CD4+ T cells, further implying that cAMP has divergent effects on Th subset differentiation (Supplemental Figure 5, B and C). Collectively, these data indicate that *Gnas*$^{\Delta CD4}$ CD4+ T cells lack normal Th17 and Th1 differentiation as a result of reduced cAMP accumulation.

Transcriptional regulation of Th17 differentiation in Gnas$^{\Delta CD4}$ *CD4+ T cells*. The reduced number of IL-17+ cells from *Gnas*$^{\Delta CD4}$ CD4+ T cells (Figure 4) and the restoration of IL-17 production by 8Br-cAMP (Figure 5) might imply that cAMP regulates the expression of transcription factors involved in Th17 differentiation (14). However, the presence of 8Br-cAMP produced no significant changes in the mRNA levels of *Rorc* (15), *Rorα*, or aryl-hydrocarbon receptor (*Ahr*) under either IL-6/TGF-β or IL-6/IL-23/IL-1β polarization conditions (Supplemental Figure 6, A–C). The expression of *Rorc* mRNA in WT and *Gnas*$^{\Delta CD4}$ CD4+ T cells was comparable during Th17 differentiation (Supplemental Figure 7A), even though the mRNA level of *Il17a* was reduced in *Gnas*$^{\Delta CD4}$ CD4+ T cells (Supplemental Figure 7B).

Since the phosphorylation of Stat3 by IL-6 or IL-23 is mandatory for Th17 differentiation, we investigated its phosphorylation in WT and *Gnas*$^{\Delta CD4}$ CD4+ T cells (16, 17). As shown in Supplemental Figure 8, we found elevated levels of Stat3 phosphorylation in *Gnas*$^{\Delta CD4}$ CD4+ T cells under each Th17 differentiation condition. We conclude that the lower number of IL-17+ cells among *Gnas*$^{\Delta CD4}$

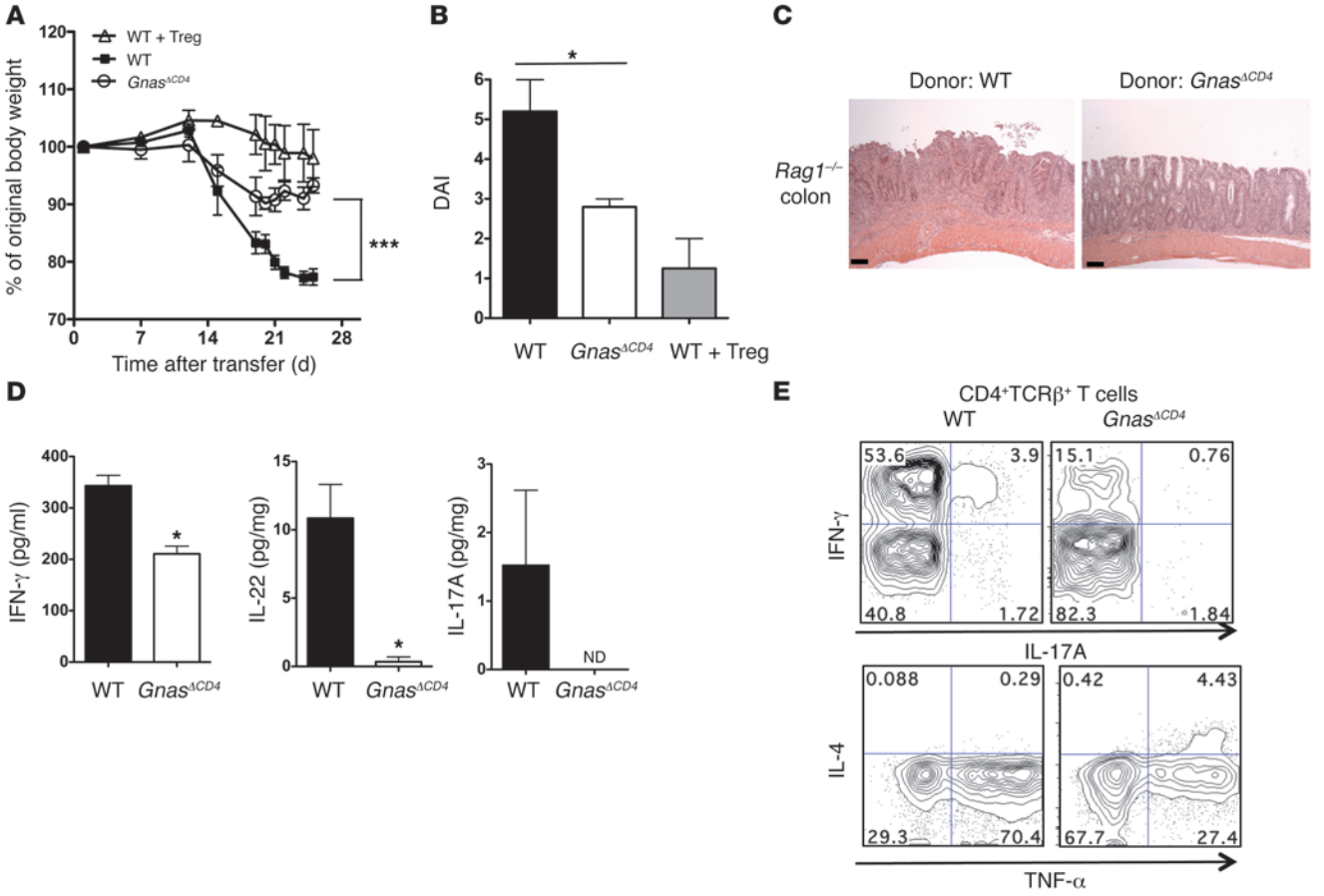

Figure 3

Gnas$^{\Delta CD4}$ CD4$^+$ T cells fail to induce colitis. (**A**) Percentage of initial body weight of *Rag1*$^{-/-}$ recipients transferred with WT or *Gnas*$^{\Delta CD4}$ FACS-sorted naive CD45RB^{hi}CD25$^-$ CD4$^+$ T cells with or without the cotransfer of CD4$^+$CD45RB^{lo}CD25$^+$ Tregs; ***$P < 0.001$, between recipients receiving WT and *Gnas*$^{\Delta CD4}$ naive CD4$^+$ T cells, by 2-way ANOVA. (**B**) Disease activity index (DAI) in recipient mice. (**C**) Minimal histological inflammation in the colons of recipients of transferred naive *Gnas*$^{\Delta CD4}$ CD4$^+$ T cells compared with severe inflammation in the colons of recipients of transferred naive WT CD4$^+$ T cells (original magnification, ×50, scale bars: 100 μM). (**D**) Cytokine levels in colon explant supernatants after 24 hours of culture. (**E**) Reduced IFN-γ$^+$ and IL-17A$^+$ CD4$^+$ T cells in *Gnas*$^{\Delta CD4}$ donor CD4$^+$ T cells. Enriched CD4$^+$ T cells from spleens of recipient mice at day 30 after transfer were stimulated with PMA/ionomycin for 4 hours. Intracellular cytokine levels were determined by flow cytometry. The number in each quadrant indicates the frequency of cells. Representative plots from 2 similar experiments are shown. Data in **A**, **B**, and **D** represent mean ± SEM from an experiment representative of 3 independent experiments with similar results. *$P < 0.05$.

CD4$^+$ T cells that was observed with Th17 polarization conditions was not due to an inhibition of RORγt expression or Stat3 activation during the Th17 differentiation program.

cAMP, via PKA, increases Ca^{2+} *influx and promotes Th17 differentiation.* Since Ca^{2+} influx is mandatory for TCR signaling and is regulated by cAMP in a number of cell types, we investigated whether Ca^{2+} had a role in the phenotype of *Gnas*$^{\Delta CD4}$ CD4$^+$ T cells (18). TCR stimulation increased cAMP levels in CD4$^+$ T cells, implying a physiological role for cAMP in T cell activation (Supplemental Figure 9). Ca^{2+} influx was reduced in *Gnas*$^{\Delta CD4}$ CD4$^+$ T cells compared with WT CD4$^+$ T cells (Figure 6A); this reduction could be reversed by addition of 8Br-cAMP (Figure 6, B and C). The Ca^{2+} transport ATPase of intracellular store–operated Ca^{2+} channels (SERCA) is inhibited by thapsigargin (Tg) (12). Treatment with Tg did not alter intracellular Ca^{2+} levels in CD4$^+$ T cells incubated in Ca^{2+}-free medium (Figure 6D); however, upon Ca^{2+} addition, Ca^{2+} influx increased to a greater extent in WT CD4$^+$ T cells than in *Gnas*$^{\Delta CD4}$ CD4$^+$ T cells. These data imply that cAMP mediates Ca^{2+} influx in CD4$^+$ T cells, especially because we observed no differences in the mRNA expression of *Orai13*, *Stim1* and *Stim2*, or L-type Ca^{2+} channels between WT and *Gnas*$^{\Delta CD4}$ CD4$^+$ T cells (Supplemental Figure 10 and refs. 12, 19).

To determine whether the cAMP-mediated increase in Ca^{2+} influx is required for Th17 differentiation, we incubated FACS-sorted naive CD4$^+$ T cells from WT and *Gnas*$^{\Delta CD4}$ mice under Th17 polarization conditions (IL-6/TGF-β) with 8Br-cAMP in the presence or absence of the L-type Ca^{2+} channel blocker diltiazem (20). Diltiazem inhibited the increase in the number of Th17$^+$ cells stimulated by 8Br-cAMP in both WT and *Gnas*$^{\Delta CD4}$ CD4$^+$ T cells (Figure 6E). The increase in Ca^{2+} influx by cAMP is PKA dependent (21): Figure 7, A and B, shows that the PKA inhibitor H-89 reduced Ca^{2+} influx and the number of IL-17$^+$ cells induced by 8Br cAMP in CD4$^+$ T cells under Th17 polarization conditions (IL-6/TGF-β). These data thus highlight a role for cAMP/PKA/Ca^{2+} in Th17 subset differentiation that is independent of lineage commitment factors, such as RORγt.

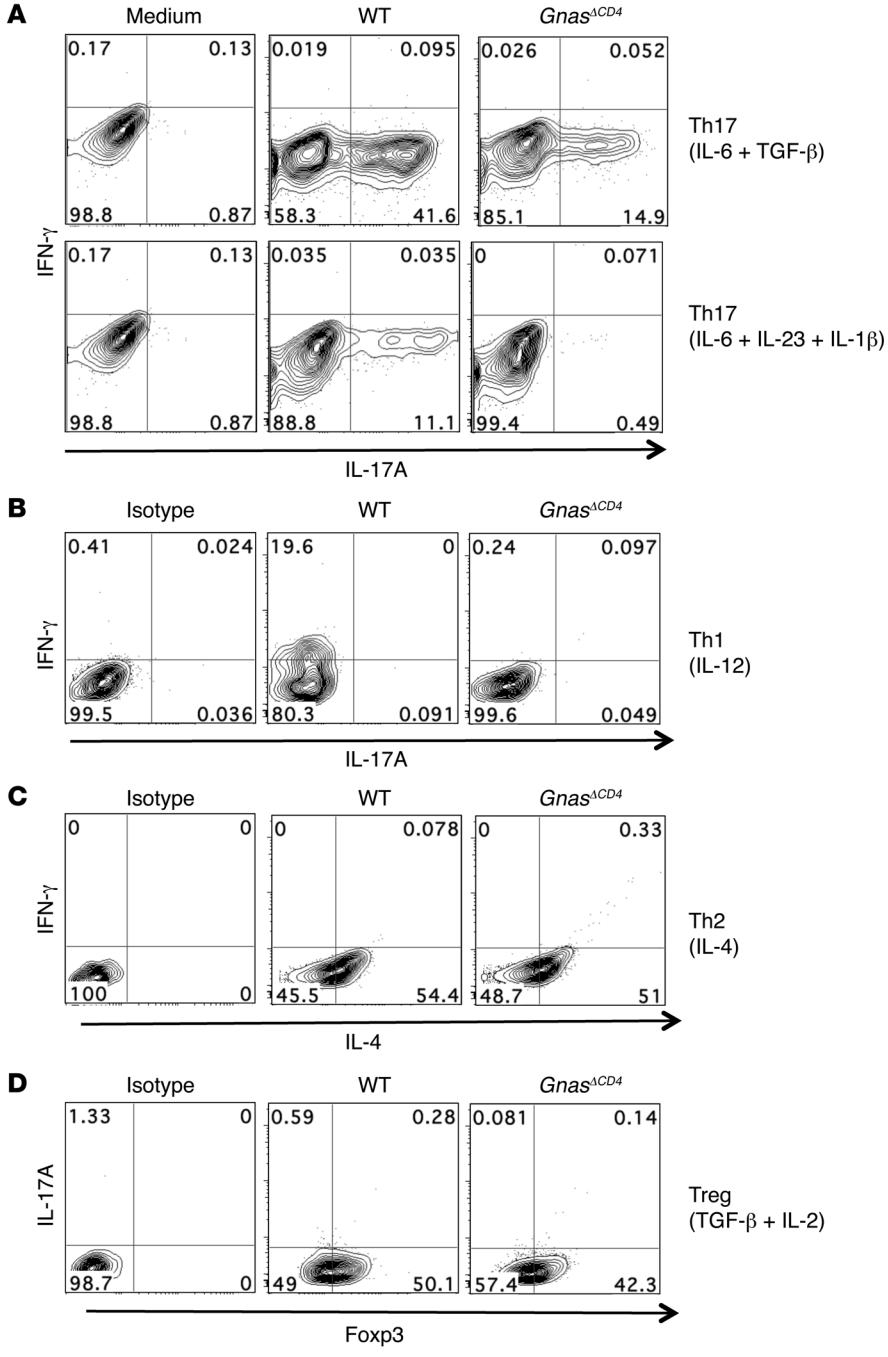

Figure 4
Reduced Th17 and Th1 cell differentiation of *Gnas*$^{\Delta CD4}$ naive CD4$^+$ T cells in vitro. FACS-sorted naive CD4$^+$ T cells from WT or *Gnas*$^{\Delta CD4}$ spleens were cultured for 4 days under Th polarization conditions for (**A**) Th17, (**B**) Th1, (**C**) Th2, and (**D**) Tregs as described in Methods. The CD4$^+$ T cells were then stimulated with PMA/ionomycin for 4 hours. IL-17A, IFN-γ, IL-4, and Foxp3 levels were determined by flow cytometry. The number in each quadrant indicates the frequency of cells. Data are representative of 3 experiments with similar results.

cAMP enhances the colitogenicity of in vitro differentiated Th17 cells. To assess the in vivo effect of cAMP on Th17 cells, we transferred WT Th17 cells that were differentiated in vitro under IL-6/TGF-β and IL-6/IL-23/IL-1β conditions in the absence or presence of 8Br-cAMP into *Rag1*$^{-/-}$ mice (Figure 8A and Supplemental Figure 11A). We then assessed the recipients over a 4-week period. *Rag1*$^{-/-}$ mice that received Th17 cells that had been differentiated in the presence of 8Br-cAMP developed more severe colitis compared with those that received Th17 cells differentiated without 8Br-cAMP (Figure 8, B and D, and Supplemental Figure 11, B and D). Consistent with previous reports of Th17 plasticity (22), CD4$^+$ T cells isolated from the mesenteric lymph nodes and spleens of recipients displayed a phenotype different from that observed prior to their transfer. The in vitro differentiation of CD4$^+$ T cells in the presence of 8Br-cAMP resulted (after transfer) in a lower percentage of IL-17$^+$ cells, but a higher percentage of IFN-γ$^+$ cells and IL-17$^+$IFN-γ$^+$ double-positive cells (Figure 8C and Supplemental Figure 11, A and C). These results highlight the proinflammatory role of cAMP in CD4$^+$ T cells and its ability to increase the colitogenic properties of Th17 cells.

Discussion

Gαs mediates the activation of AC and generation of cAMP in response to GPCR agonists (1). Global Gαs deficiency is embryonically lethal; therefore, we generated mice with a T cell–selective deletion of Gαs (8, 23, 24). *Gnas*$^{\Delta CD4}$ CD4-Cre mice developed normally, but their CD4$^+$ T cells did not accumulate cAMP; had reduced Ca^{2+} influx; secreted lower levels of IL-17, IL-22, and IFN-γ (but normal IL-4) compared with WT CD4$^+$ T cells; and did not mount an antigen-specific Th17 response upon CT/OVA immunization (Figure 2). The adoptive transfer of naive *Gnas*$^{\Delta CD4}$ CD4$^+$ T cells into *Rag1*$^{-/-}$ recipients provoked minimal colonic inflammation compared with that induced by the transfer of naive WT CD4$^+$ T cells. Consistent with this phenotype, *Gnas*$^{\Delta CD4}$ CD4$^+$ T cells isolated from recipients' spleens displayed a lower frequency of IFN-γ$^+$, IFN-γ$^+$IL-17$^+$, and TNF-α$^+$ cells. To better elucidate the role of Gαs in Th cell differentiation, we used an in vitro differentiation system. CD4$^+$ T cells from *Gnas*$^{\Delta CD4}$ mice displayed fewer Th17 and Th1 cells but comparable expression of Th2 or Tregs relative to WT CD4$^+$ T cells (Figure 4). Collectively, these in vitro and in vivo data indicate a divergent role for Gαs in Th subset differentiation and function.

To determine whether the phenotype of *Gnas*$^{\Delta CD4}$ CD4$^+$ T cells was the result of reduced cAMP accumulation, we used 8Br-cAMP to restore cAMP levels and assessed in vitro Th differentiation. 8Br-cAMP restored the expression of *Gnas*$^{\Delta CD4}$ IL-17$^+$ and IFN-γ$^+$ but did not alter IL-4$^+$ or Foxp3$^+$ CD4$^+$ T cells, implying that reduced

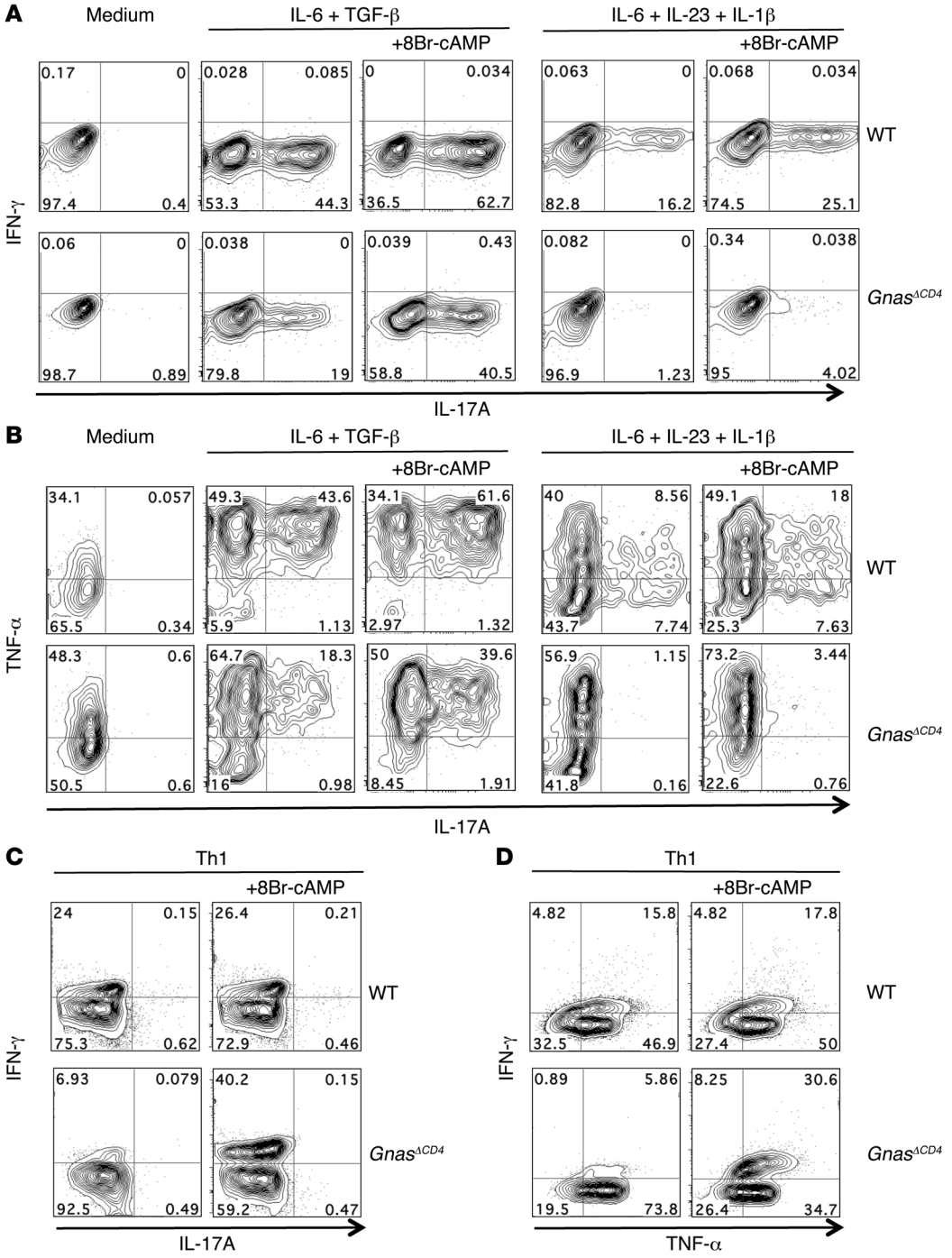

Figure 5
cAMP restores Th17 and Th1 differentiation of *Gnas*$^{\Delta CD4}$ CD4$^+$ T cells. (**A** and **B**) FACS-sorted naive CD4$^+$ T cells from WT or *Gnas*$^{\Delta CD4}$ spleens were cultured for 4 days under two Th17 polarization conditions: IL-6/TGF-β or IL-6/IL-23/IL-1β with or without 8Br-cAMP (25 μM). (**C** and **D**) FACS-sorted naive CD4$^+$ T cells were cultured for 4 days under Th1 polarization conditions with or without 8Br-cAMP (25 μM). The CD4$^+$ T cells were stimulated with PMA/ionomycin for 4 hours, and the intracellular levels of IL-17A, IFN-γ, and TNF-α were determined by FACS analysis. The number in each quadrant indicates the frequency of cells. The data are representative of 3 independent experiments with similar results.

cAMP accumulation in *Gnas*$^{\Delta CD4}$ CD4$^+$ T cells selectively modulates Th17 and Th1 differentiation. Furthermore, restoring cAMP increased the expression of IL-17$^+$TNF-α$^+$ and IFN-γ$^+$TNF-α$^+$ cells, demonstrating that cAMP enhances the inflammatory phenotype of Th17 and Th1 subsets (Figure 5). The 8Br-cAMP–promoted Th17 phenotype observed in CD4$^+$ T cells from *Gnas*$^{\Delta CD4}$ mice was not associated with increased levels of Th17 lineage-specific transcription factors (Supplemental Figures 7 and 8), thus indicating that a transcriptional defect does not account for the impairment in Th17 differentiation.

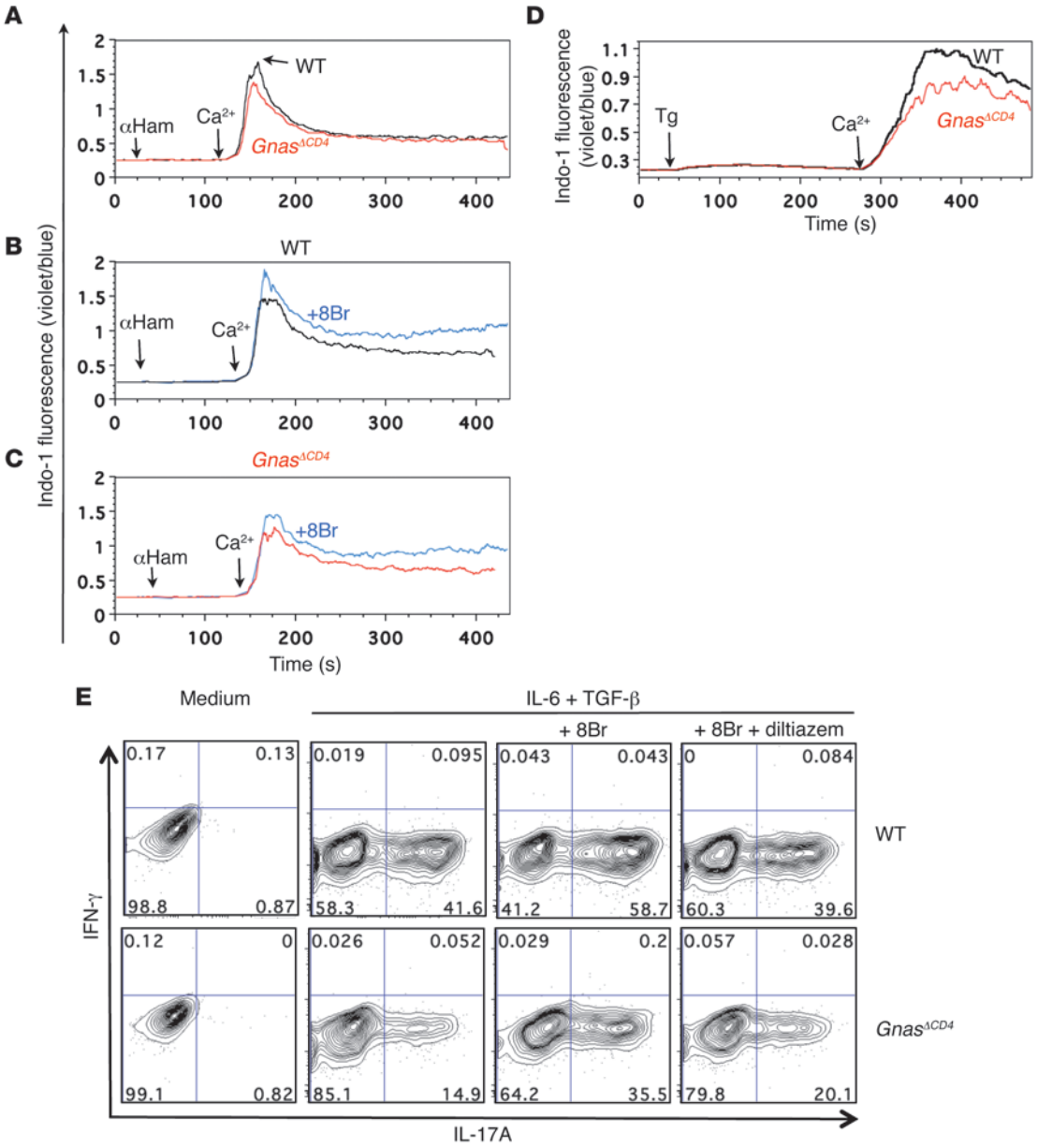

Figure 6

cAMP, via increasing Ca^{2+} influx, restores Th17 and Th1 differentiation of $Gnas^{\Delta CD4}$ $CD4^+$ T cells. (**A**–**C**) Ca^{2+} influx in enriched WT or $Gnas^{\Delta CD4}$ splenic $CD4^+$ T cells. $CD4^+$ T cells stained with anti-CD3 Ab were cross-linked with goat anti-hamster Abs (αHam) in Ca^{2+}-free HBSS medium, followed by the addition of $CaCl_2$ (2 mM); WT (CFSE-labeled) or $Gnas^{\Delta CD4}$ $CD4^+$ T cells (no label) were mixed, incubated with the calcium indicator Indo-1 AM, and assayed in one tube at the same time in the same environment. Ca^{2+} influx was measured by changes in the mean fluorescence ratio of Indo-1 AM at violet (405 nm) to blue laser (510 nm). 8Br, 8Br-cAMP, 25 μM. The data are representative of 1 of 3 independent experiments. (**D**) Reduced Ca^{2+} influx in $Gnas^{\Delta CD4}$ splenic $CD4^+$ T cells stimulated by Tg. WT or $Gnas^{\Delta CD4}$ splenic $CD4^+$ T cells in Ca^{2+}-free HBSS medium (EGTA, 0.5 mM) were stimulated by Tg (1 μM), followed by the addition of $CaCl_2$ (2 mM). (**E**) Diltiazem inhibits the 8Br-cAMP increase in Th17 cells. FACS-sorted naive $CD4^+$ T cells were cultured for 4 days under Th17 differentiation conditions (IL-6/TGF-β) as indicated. 8Br: 25 μM; diltiazem: 20 μM. The $CD4^+$ T cells were stimulated with PMA/ionomycin for 4 hours. Intracellular cytokine levels were determined by flow cytometry. The number in each quadrant indicates the frequency of cells. Data are representative of 2 independent experiments with similar results.

In addition to the expression of lineage-specific transcription factors, differentiation of Th17 or Th1 cells is regulated by Ca^{2+} signaling, with Ca^{2+} influx primarily mediated by calcium release–activated channels (CRACs), inositol-1,4,5-trisphosphate receptors (IP_3Rs), and L-type calcium channels (25, 26). Defective CRACs or L-type calcium channels in $CD4^+$ T cells can inhibit Th17 and Th1 cell differentiation without inhibiting the expression of RORγt or T-bet (12). Since cAMP can activate L-type calcium channels (27), we postulated that $Gnas^{\Delta CD4}$ $CD4^+$ T cells have reduced Ca^{2+} influx that contributes to their Th phenotype. Indeed, we found that com-

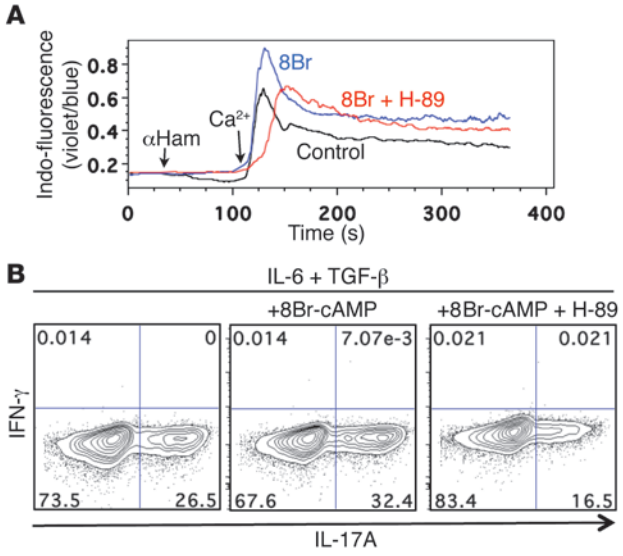

Figure 7

cAMP, via PKA, increases Ca^{2+} influx and promotes Th17 differentiation. (**A**) cAMP-mediated Ca^{2+} influx in WT $CD4^+$ T cells is inhibited by PKA. $CD4^+$ T cells stained with anti-CD3 Ab were crosslinked with goat anti-hamster Abs (αHam) in Ca^{2+}-free HBSS medium, followed by the addition of $CaCl_2$ (2 mM); H-89: 10 μM, 15 minutes preincubation; 8Br-cAMP, 25 μM. (**B**) cAMP promotes Th17 differentiation via PKA. FACS-sorted naive WT $CD4^+$ T cells were cultured for 4 days under Th17 differentiation conditions (IL-6/TGF-β) with the indicated reagents. H-89: 10 μM, 30 minutes preincubation. The number in each quadrant indicates the frequency of cells. Data are representative 3 independent experiments with similar results.

pared with WT $CD4^+$ T cells, $Gnas^{\Delta CD4}$ $CD4^+$ T cells had reduced Ca^{2+} influx and a reduced Th17 polarization response and that this reduced response could be restored with 8Br-cAMP; blocking Ca^{2+} channels inhibited the increase in Th17 cell number (Figure 6). Moreover, the cAMP-induced Ca^{2+} influx and subsequent Th17 differentiation were PKA dependent (Figure 7). Previous data have suggested that Gαs can directly activate Ca^{2+} channels (28, 29) and non-receptor and receptor tyrosine kinases (30–32); however, our results indicating that addition of a cAMP analog could reverse the phenotype of the $Gnas^{\Delta CD4}$ $CD4^+$ T cells imply that the effects of Gαs on Th subset differentiation is likely to be mediated, at least for the most part, by decreased cAMP accumulation in these cells.

Our in vitro data suggested that cAMP not only promotes Th17 and Th1 differentiation but also increases their inflammatory profile. To validate this finding in vivo, we transferred Th17 cells that were differentiated in vitro with or without 8Br-cAMP into $Rag1^{-/-}$ recipients and tested their ability to provoke colitis. Adding 8Br-cAMP increased the severity of colitis and the inflammatory profile of the $CD4^+$ T cells 4 weeks after transfer (Figure 8 and Supplemental Figure 11). The adoptive transfer of $Gnas^{\Delta CD4}$ naive $CD4^+$ T cells into $Rag1^{-/-}$ recipients resulted in a lower disease activity index and reduced destruction of the colonic mucosa compared with transfer of WT $CD4^+$ T cells (Figure 3), further indicating a role for Gαs-dependent cAMP production in the induction and/or maintenance of the inflammatory $CD4^+$ T cell phenotype.

Taken together, our data show the importance of Gαs and the synthesis and accumulation of cAMP and activation of PKA in the induction of Th17 and Th1 cell differentiation, as well as in the upregulation of their inflammatory responses. Importantly, these effects were not observed for Th2 cells, thus implying that their differentiation is independent of cAMP and cAMP/PKA-induced Ca^{2+} influx. This observation is consistent with evidence that the activation of Th1 and Th2 under the same conditions results in different patterns of Ca^{2+} signaling and cytokine production (33).

Our results thus indicate that cAMP has a proinflammatory and not, as previously proposed (3), an immunosuppressive effect, in terms of regulation of the function of Th cells. A possible explanation for differences in such results is that we assessed the role of cAMP during Th cell differentiation while others evaluated such a role after differentiation of Th cells. The Th-specific effects by cAMP suggest that it may be exploited for therapeutic immunomodulation. Such therapeutic effects might be achieved by targeting: (a) cAMP formation through the activation of Gαs-coupled or inhibition of Gαi-coupled GPCRs, (b) cAMP degradation by inhibiting PDE isoforms, or (c) L-type Ca^{2+} channels through their blockade in $CD4^+$ T cells. It will be of interest to test such approaches in future studies.

Methods

Mice. C57BL/6 (B6) mice were purchased from Harlan, CD4-Cre transgenic mice from Taconic, and OT-2 (B6) mice expressing a transgenic TCR that recognize class II–derived OVA peptide and $Rag1^{-/-}$ mice (B6) from The Jackson Laboratory. To generate Gαs-deficient T cells, lox-flanked *Gnas* mice (8) were crossed to CD4-Cre mice. The T cells in the $Cre^+Gnas^{\Delta CD4}$ mice were determined to be $Gnas^{\Delta CD4}$ and $Gnas^{\Delta CD8}$. The WT littermates (Cre^- $Gnas^{fl/fl}$) or B6 mice were used as control (WT). To generate OVA-specific $Gnas^{\Delta CD4}$ mice, we crossed $Gnas^{\Delta CD4}$ to OT-2 mice. Seven- to 12-week-old mice were used in all the experiments and were maintained under specific pathogen–free conditions.

Reagents. Reagents were obtained as follows: 8Br-cAMP and PKA inhibitor H-89 from Calbiochem; recombinant cytokines (IL-23, IL-1β, and IL-6) and anti–mouse CD28 Ab from eBioscience; human recombinant TGF-β from PeproTech; IL-2 from Sigma-Aldrich; anti–mouse CD3e (clone 2C11), anti–IL-4 (clone 11B11), and anti–IFN-γ (clone XMG1.2) neutralizing antibodies from BioXcell; rolipram and diltiazem from Tocris Bioscience. Tg, forskolin, PGE_2, and isoproterenol were purchased from Sigma-Aldrich.

$CD4^+$ T cell isolation and differentiation in vitro. $CD4^+$ T cells were isolated by immunomagnetic selection (EasySep CD4-negative selection kit, StemCell Technologies) from a single-cell suspension of splenocytes or peripheral lymph node cells. Naive $CD4^+$ T cells ($CD62L^{hi}CD44^{lo}CD25^-$) were isolated from $CD4^+$ T cells by FACS sorting (Aria, BD Biosciences). Cells were incubated in complete IMDM medium (Invitrogen) supplemented with 2 mM L-glutamine, 100 U/ml penicillin, 100 μg/ml streptomycin, 50 μM β-mercaptoethanol, and 10% FCS. Culture plates (48-well) were coated with goat anti-hamster Ab (0.1 mg/ml, USBiological). Naive $CD4^+$ T cells (1×10^6/ml) were cultured in medium with soluble anti-CD3 Ab (0.25 μg/ml), anti-CD28 Ab (1 μg/ml), and neutralizing antibodies for IL-4 (10 μg/ml) and IFN-γ (10 μg/ml).

Naive $CD4^+$ T cells were differentiated into Th17 cells according to two protocols: (a) TGF-β–dependent Th17 cells were obtained by addition of IL-6 (20 ng/ml) and TGF-β (4 ng/ml) to the Th0 cultures (34); (b) IL-23–mediated Th17 differentiation by addition of IL-6 (20 ng/ml), IL-23 (10 ng/ml), and IL-1β (10 ng/ml) (13). Naive $CD4^+$ T cells were cultured in goat anti-hamster Ab–coated culture plates in complete IMDM medium with soluble anti-CD3 Ab (5 μg/ml) and anti-CD28 Ab (1 μg/ml), added with IL-12 (20 ng/ml) and neutralizing anti–IL-4 Ab (10 μg/ml) for Th1 differentiation; or IL-4 (10 ng/ml) and neutralizing anti–IFN-γ Ab (10 μg/ml) for Th2

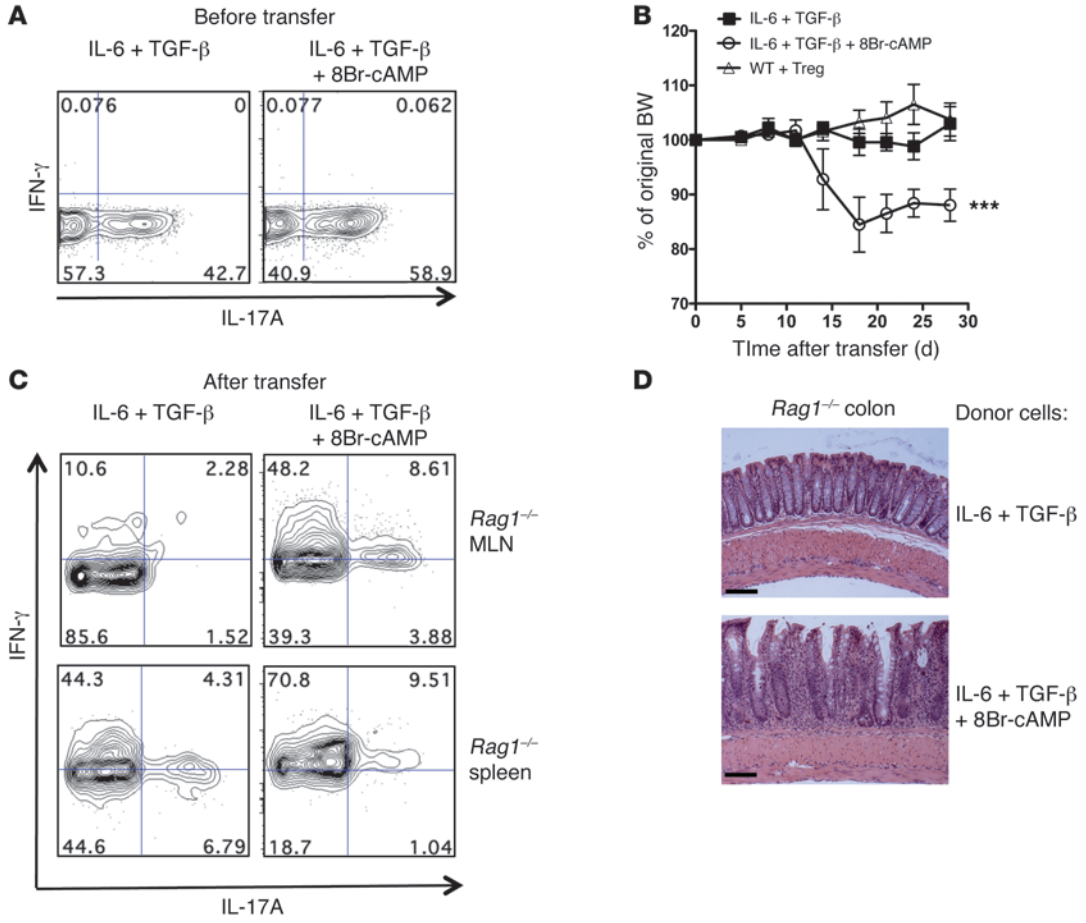

Figure 8

cAMP enhances the colitogenicity of in vitro differentiated Th17 cells. FACS-sorted naive CD4+ T cells from WT spleens were cultured for 4 days under Th17 differentiation conditions (IL-6/TGF-β) with or without 8Br-cAMP (25 μM) and then adoptively transferred into *Rag1*$^{-/-}$ mice. (**A**) Intracellular expression of IFN-γ and IL-17A in Th17 cells before transfer. (**B**) Percentage of initial body weight of *Rag1*$^{-/-}$ recipients after transfer of Th17 cells (differentiated in vitro with or without 8Br-cAMP). The co-transfer of WT CD4$^+$CD45RB^{hi}CD25$^-$ T cells with CD45RB^{lo}CD25$^+$ Tregs was used as control. Data are shown as mean ± SEM; $n = 3–5$; ***$P < 0.001$, 2-way ANOVA, recipients receiving in vitro differentiated Th17 cells with or without 8Br-cAMP. (**C**) Intracellular expression of IFN-γ and IL-17A in Th17 cells 28 days after transfer. CD4+ cells from spleen or MLN of recipient mice at day 28 after transfer were stimulated with PMA/ionomycin for 4 hours, and the intracellular cytokine levels were determined by flow cytometry. The number in each quadrant (**A** and **C**) indicates the frequency of cells. (**D**) Histological analysis of the colons of *Rag1*$^{-/-}$ mice receiving in vitro differentiated Th17 cells with or without 8Br-cAMP (original magnification, ×100, scale bars: 100 μM).

differentiation. At day 2, recombinant human IL-2 (20 U/ml) was added into the Th1 or Th2 culture. For Treg differentiation, TGF-β (10 ng/ml) and IL-2 (100 U/ml) were added into IMDM culture medium. After 4 days, cells were collected for analysis.

ELISA measurement of cytokines. Splenic CD4+ T cells were enriched by immunomagnetic cell selection (EasySep CD4 negative selection kit, StemCell Technologies) to greater than 95% purity by negative selection. CD4+ T cells (1×10^5 cells) were stimulated with plate-bound anti-CD3 Ab (10 μg/ml) and anti-CD28 Ab (1 μg/ml) for 72 hours in complete RPMI medium (Mediatech Inc.) supplemented with 2 mM L-glutamine, 100 U/ml penicillin, 100 μg/ml streptomycin, 50 μM β-mercaptoethanol, and 10% FCS. Cytokine levels in the supernatant were determined using ELISA kits for IL-17A, IL-5, IL-10, TNF-α, IFN-γ (eBioscience), and IL-22 (Antigenix America Inc.) following the manufacturers' instructions.

Flow cytometry and intracellular staining. All antibodies used for cell labeling were purchased from BD Biosciences — Pharmingen and eBiosciences. The data were acquired by an LSR II, FACSCalibur, and C6 Accuri flow cytometer (BD Biosciences) and analyzed by FlowJo software (Tree Star Inc.). For measurements of intracellular cytokines, CD4+ T cells were stimulated with PMA (50 ng/ml) and ionomycin (1 μM) in the presence of GolgiStop (BD Biosciences — Pharmingen) for 4 hours. Cytokines were analyzed using antibodies to IL-17A, TNF-α, IL-4, Foxp3, or IFN-γ (eBioscience) according to the manufacturer's instructions. For measurements of p-Stat3 levels, we incubated CD4+ T cells with anti-CD3 (10 μg/ml) and anti-CD28 (1 μg/ml) Abs with the indicated cytokines for 15 minutes. Cells were fixed by 1.5% formaldehyde, 100% methanol, and stained by anti–p-Stat3–PE Ab (pY705, BD Biosciences — Pharmingen).

cAMP assay. cAMP accumulation was measured as previously described (35). CD4+ T cells or CD11c+ BMDCs were enriched by magnetic selection and equilibrated in RPMI-1640 medium containing 10% FCS for 30 minutes at 37°C and then incubated with stimulatory agonists for 10 minutes in the absence and presence of PDE inhibitors (added 30 minutes before the addition of agonists). Reactions were terminated by aspiration of the

medium and addition of 50 μl of cold 7.5% (wt/vol) trichloroacetic acid (TCA) per million cells. cAMP content in TCA extracts was determined by radioimmunoassay and normalized to the amount of cells per well.

OVA-specific immune responses upon in vitro immunization. Naive OT-2 $CD4^+$ T cells from spleens of WT or $Gnas^{\Delta CD4}$ mice were enriched by immunomagnetic cell selection (EasySep CD4 negative selection kit, StemCell Technologies) to greater than 95% purity and were further depleted of $CD25^+$ cells (anti-CD25 Biotin Ab and Biotin selection kit, StemCell Technologies) by negative selection. The WT splenic DCs were isolated by use of a CD11c positive selection kit (StemCell Technologies). DCs (0.5×10^6) were then cocultured with WT or OT-2/$Gnas^{\Delta CD4}$ naive T cells (1×10^6) in RMPI-1640 medium in the presence of class II OVA peptide (aa 323–339) (10 μg/ml) for 5 days. OT-2 cells (1×10^5) were then collected and stimulated by plate-bound anti-CD3 Ab (10 μg/ml) and soluble anti-CD28 Ab (1 μg/ml) for 24 hours. Supernatants were collected and cytokine levels were determined (ELISA).

Oral CT/OVA immunization. Mice were immunized orally by gavage on day 0 and day 14 with CT (20 μg, List Laboratories) and OVA (200 μg, Sigma-Aldrich), as described previously (7). On day 39, the mice were challenged with OVA (200 μg i.p.). Single-cell suspensions from spleens were collected on day 42 and incubated for 3 days with medium alone or supplemented with OVA (200 μg/ml). The concentration of cytokines in the supernatants was determined by ELISA.

Ca^{2+} flux measurement. Splenic $CD4^+$ T cells were loaded for 10 minutes at 37°C with CFSE (20 nM), followed by washing. Equal numbers of CFSE-labeled WT $CD4^+$ T cells were mixed with the unlabeled $Gnas^{\Delta CD4}$ $CD4^+$ T cells. Cells were suspended at a density of 1×10^7 cells per ml in Ca^{2+}-free and Mg^{2+}-free HBSS supplemented with 2% FCS and incubated for 1 hour at 37°C in 5% CO_2 with the calcium indicator Indo-1 AM (36) (2 μM; Molecular Probes, Invitrogen). Cells were washed with HBSS medium and were treated for 30 minutes on ice with anti-CD3 (clone 2C11) Ab and APC-conjugated anti-CD4 Ab (GK1.5, eBioscience). Cells were washed once with HBSS, placed on ice for 1 hour, and rewarmed to 37°C before data analysis on an LSR II (BD). For cell stimulation, goat anti-hamster Ab (5 μg/ml) was added to crosslink CD3 Abs. $CaCl_2$ (2 mM) and 8Br-cAMP (50 μM) were added as indicated. In some experiments, $CD4^+$ T cells were preincubated with the PKA inhibitor H-89 (10 μM) for 15 minutes at 37°C. The data are presented as the ratio of violet (405 nm) to blue (510 nm) Indo-1 fluorescence and were calculated using FlowJo (Tree Star Inc.).

Adoptively transferred $CD4^+$ T cells induced colitis. Colitis was induced by adoptive transfer of naive $CD45RB^{hi}$ $CD4^+$ T cells: sorted naive $CD4^+$ T cells ($CD4^+CD45RB^{hi}CD25^-$, 1×10^5 cells/mouse) from WT or $Gnas^{\Delta CD4}$ spleen were adoptively transferred into 12-week-old sex- and age-matched $Rag1^{-/-}$ mice as described previously (37). A group of $Rag1^{-/-}$ mice also received 0.5×10^5 $CD45RB^{lo}CD25^+$ (Tregs) from WT mice; naive $CD4^+$ T cells (1×10^5 cells) were used controls. After transfer, mice were monitored for weight loss and signs of intestinal inflammation. Diseased animals were sacrificed for analysis between 4 and 6 weeks after transfer. Splenic and mesenteric lymph node (MLN) cells were cultured in RPMI-1640 medium and stimulated by PMA/ionomycin for 5 hours in the presence of GolgiStop (BD Biosciences — Pharmingen) for intracellular staining. The colon explants were isolated and cultured as described previously (37), and cytokines levels in the supernatant were measured (ELISA).

Histological evaluation of colitis. The colon was excised, opened longitudinally, rolled onto a wooden stick, fixed with 10% neutral buffered formaldehyde solution, and embedded in paraffin. Tissue sections (5 μm) were prepared, deparaffinized, and stained with H&E. Sections were analyzed in a blinded fashion as described in previous studies (37).

Quantitative PCR analysis. Isolation of RNA was carried out using an RNeasy Mini Kit (QIAGEN) according to the manufacturer's instructions. The cDNA was synthesized using Superscript III First-Strand system (Invitrogen). Quantitative PCR analysis was performed as described previously (37). SYBR Green PCR Master Mix was used for real-time PCR (7300 system, Applied Biosystems). Samples were run in duplicate or triplicate and normalized by a housekeeping gene (mouse *Rplp0* and mouse *18s* rRNA). The primer sequences are provided in Supplemental Table 1.

Statistics. Data are presented as mean ± SEM. Unpaired Student's *t* test with 2-tailed *P* values was used for statistical analyses unless indicated otherwise (GraphPad Prism software). In all tests, *P* values less than 0.05 were considered statistically significant.

Study approval. All experimental procedures were approved by the UCSD IACUC.

Acknowledgments

We thank Liang Zhou, Dianel Mucida, Jongdae Lee, and Nakon Aroonsakool for technical help and discussion. This study was supported by NIH grants AI068685, AI095623, AI077989, DK35108, DK080506, and T32 AI7469 and a grant from the Crohn's and Colitis Foundation of America.

Received for publication May 19, 2011, and accepted in revised form January 4, 2012.

Address correspondence to: Eyal Raz, Department of Medicine 0663, University of California San Diego, La Jolla, California 92093-0663, USA. Phone: 858.534.5444; Fax: 858.534.0409; E-mail: eraz@ucsd.edu.

1. Weinstein LS, Liu J, Sakamoto A, Xie T, Chen M. Minireview: GNAS: normal and abnormal functions. *Endocrinology*. 2004;145(12):5459–5464.
2. Bender AT, Beavo JA. Cyclic nucleotide phosphodiesterases: molecular regulation to clinical use. *Pharmacol Rev*. 2006;58(3):488–520.
3. Mosenden R, Taskén K. Cyclic AMP-mediated immune regulation — overview of mechanisms of action in T cells. *Cell Signal*. 2011;23(6):1009–1016.
4. Yao C, et al. Prostaglandin E2-EP4 signaling promotes immune inflammation through Th1 cell differentiation and Th17 cell expansion. *Nat Med*. 2009; 15(6):633–640.
5. Napolitani G, Acosta-Rodriguez EV, Lanzavecchia A, Sallusto F. Prostaglandin E2 enhances Th17 responses via modulation of IL-17 and IFN-gamma production by memory $CD4^+$ T cells. *Eur J Immunol*. 2009;39(5):1301–1312.
6. Boniface K, et al. Prostaglandin E2 regulates Th17 cell differentiation and function through cyclic AMP and EP2/EP4 receptor signaling. *J Exp Med*. 2009;206(3):535–548.
7. Datta SK, et al. Mucosal adjuvant activity of cholera toxin requires Th17 cells and protects against inhalation anthrax. *Proc Natl Acad Sci U S A*. 2010; 107(23):10638–10643.
8. Chen M, et al. Increased glucose tolerance and reduced adiposity in the absence of fasting hypoglycemia in mice with liver-specific Gs alpha deficiency. *J Clin Invest*. 2005;115(11):3217–3227.
9. Darfler FJ, Mahan LC, Koachman AM, Insel PA. Stimulation of forskolin of intact S49 lymphoma cells involves the nucleotide regulatory protein of adenylate cyclase. *J Biol Chem*. 1982; 257(20):11901–11907.
10. Brand S. Crohn's disease: Th1, Th17 or both? The change of a paradigm: new immunological and genetic insights implicate Th17 cells in the pathogenesis of Crohn's disease. *Gut*. 2009;58(8):1152–1167.
11. Liu ZJ, Yadav PK, Su JL, Wang JS, Fei K. Potential role of Th17 cells in the pathogenesis of inflammatory bowel disease. *World J Gastroenterol*. 2009;15(46):5784–5788.
12. Ma J, McCarl CA, Khalil S, Lüthy K, Feske S. T-cell-specific deletion of STIM1 and STIM2 protects mice from EAE by impairing the effector functions of Th1 and Th17 cells. *Eur J Immunol*. 2010; 40(11):3028–3042.
13. Ghoreschi K, et al. Generation of pathogenic T(H)17 cells in the absence of TGF-beta signalling. *Nature*. 2010;467(7318):967–971.
14. Zhou L, Littman DR. Transcriptional regulatory networks in Th17 cell differentiation. *Curr Opin Immunol*. 2009;21(2):146–152.
15. Ivanov II, et al. The orphan nuclear receptor RORgammat directs the differentiation program of proinflammatory IL-17+ T helper cells. *Cell*. 2006; 126(6):1121–1133.
16. Durant L, et al. Diverse targets of the transcription factor STAT3 contribute to T cell pathogenicity and homeostasis. *Immunity*. 2010;32(5):605–615.
17. Yang XO, et al. STAT3 regulates cytokine-mediated generation of inflammatory helper T cells.

J Biol Chem. 2007;282(13):9358–9363.
18. McCarl CA, et al. Store-operated Ca2+ entry through ORAI1 is critical for T cell-mediated autoimmunity and allograft rejection. *J Immunol*. 2010; 185(10):5845–5858.
19. Matza D, Flavell RA. Roles of Ca(v) channels and AHNAK1 in T cells: the beauty and the beast. *Immunol Rev*. 2009;231(1):257–264.
20. Kesten KS, Reuter NS, Swisher JD. Diltiazem: the latest calcium-channel blocker. *Dimens Crit Care Nurs*. 1984;3(3):154–160.
21. Conche C, Boulla G, Trautmann A, Randriamampita C. T cell adhesion primes antigen receptor-induced calcium responses through a transient rise in adenosine 3′,5′-cyclic monophosphate. *Immunity*. 2009;30(1):33–43.
22. Zhou L, Chong MM, Littman DR. Plasticity of CD4+ T cell lineage differentiation. *Immunity*. 2009; 30(5):646–655.
23. Adams GB, et al. Haematopoietic stem cells depend on Galpha(s)-mediated signalling to engraft bone marrow. *Nature*. 2009;459(7243):103–107.
24. Weinstein LS. Gs alpha knockouts in mice and man. *Rinsho Byori*. 1999;47(5):425–429.
25. Matza D, et al. A scaffold protein, AHNAK1, is required for calcium signaling during T cell activation. *Immunity*. 2008;28(1):64–74.
26. Oh-hora M. Calcium signaling in the development and function of T-lineage cells. *Immunol Rev*. 2009;231(1):210–224.
27. Hell JW. Beta-adrenergic regulation of the L-type Ca2+ channel Ca(V)1.2 by PKA rekindles excitement. *Sci Signal*. 2010;3(141):pe33.
28. Yatani A, Imoto Y, Codina J, Hamilton SL, Brown AM, Birnbaumer L. The stimulatory G protein of adenylyl cyclase, Gs, also stimulates dihydropyridine-sensitive Ca2+ channels. Evidence for direct regulation independent of phosphorylation by cAMP-dependent protein kinase or stimulation by a dihydropyridine agonist. *J Biol Chem*. 1988; 263(20):9887–9895.
29. Mattera R, et al. Splice variants of the alpha subunit of the G protein Gs activate both adenylyl cyclase and calcium channels. *Science*. 1989;243(4892):804–807.
30. Nair BG, Parikh B, Milligan G, Patel TB. Gs alpha mediates epidermal growth factor-elicited stimulation of rat cardiac adenylate cyclase. *J Biol Chem*. 1990; 265(34):21317–21322.
31. Poppleton H, Sun H, Fulgham D, Bertics P, Patel TB. Activation of Gsalpha by the epidermal growth factor receptor involves phosphorylation. *J Biol Chem*. 1996;271(12):6947–6951.
32. Sun H, et al. The juxtamembrane, cytosolic region of the epidermal growth factor receptor is involved in association with alpha-subunit of Gs. *J Biol Chem*. 1997;272(9):5413–5420.
33. Weber KS, Miller MJ, Allen PM. Th17 cells exhibit a distinct calcium profile from Th1 and Th2 cells and have Th1-like motility and NF-AT nuclear localization. *J Immunol*. 2008;180(3):1442–1450.
34. Zhou L, et al. IL-6 programs T(H)-17 cell differentiation by promoting sequential engagement of the IL-21 and IL-23 pathways. *Nat Immunol*. 2007; 8(9):967–974.
35. Murray F, et al. Expression and activity of cAMP phosphodiesterase isoforms in pulmonary artery smooth muscle cells from patients with pulmonary hypertension: role for PDE1. *Am J Physiol Lung Cell Mol Physiol*. 2007;292(1):L294–L303.
36. Fu G, Gascoigne NR. Multiplexed labeling of samples with cell tracking dyes facilitates rapid and accurate internally controlled calcium flux measurement by flow cytometry. *J Immunol Methods*. 2009; 350(1–2):194–199.
37. Gonzalez-Navajas JM, et al. TLR4 signaling in effector CD4+ T cells regulates TCR activation and experimental colitis in mice. *J Clin Invest*. 2010; 120(2):570–581.